10th World Congress on Structural and Multidisciplinary Optimization
May 19 - 24, 2013, Orlando, Florida, USA

Design of a far-infrared lens based on topology optimization

Yuya Akatsuchi[1], Takayuki Yamada[2], Kazuhiro Izui[2], Shinji Nishiwaki[2],Makoto Ohkado[3], Tsuyoshi Nomura[3]

[1] Kyoto University, Kyoto, Japan, akatsuchi.yuya.88x@st.kyoto-u.ac.jp
[2] Kyoto University, Kyoto, Japan,
[3] Toyota Central R&D Labs, Inc, Aichi, Japan

1. Abstract
This paper proposes a design methodology for the topology optimization of a far-infrared single-element lens. The far-infrared lenses used in far-infrared cameras determine the basic performance of such devices, such as their angle of view, resolution, and so on. However, the design of far-infrared-lenses still mainly depends on trial and error approaches and the experience and intuition of skilled designers, hence the desirability of a systematic method for lens design. Topology optimization methods, the most flexible type of structural optimization methods, are especially useful in this case. Topology optimization techniques have been extended to electromagnetic wave propagation problems that are relevant to lens design problems. In typical lens design topology optimization approaches, however, the focal point is set relatively near the fixed design domain and almost always lies within the analysis region, and viewing angles and resolutions are not taken into account. In this study, we propose a new far-infrared lens design method using topology optimization in which the directivity in the far-field is optimized by using the electric field distribution in the near-field, which enables the optimal design of lenses only given a desired directivity pattern. Here, to verify the effectiveness of the proposed method, we optimize a light collimator. The optimization algorithm uses the finite element method (FEM) for solving the equilibrium and adjoint equations, and the design problem is formulated for a two-dimensional case. We first introduce the concept and scheme of the proposed topology optimization method. Next, the optimization problem for the design of a far-infrared lens is formulated. Finally, numerical examples of optimally designed far-infrared lens structures are presented.
2. Keywords: topology optimization, far-infrared lens, far-field, silicon.

3. Introduction

In recent years, the use of far-infrared cameras for night-time security applications and in automotive pedestrian detection systems has been extensively promoted [1][2][3]. Conventional pedestrian detection sensors typically use near-infrared cameras that require laser illumination, but far-infrared cameras offer several advantages, such as the ability to directly detect the heat radiated by people without the need for a separate infrared source, and the possibility of developing simpler systems. Moreover, far-infrared systems are not affected by fog or rain. A far-infrared camera is composed of a lens and a sensor, but basic performances such as the angle of view, resolution, and so on, are determined by the design of the lens. Despite the use of various aids when designing lenses, trial and error approaches and dependence on the experience and intuition of skilled designers are still common, hence the desirability of a systematic method for lens design.

In this case, a topology optimization method is particularly useful because it is the most flexible type of structural optimization method and is based on mathematical principles. Changes in both the shape and the number of holes in structures can occur as structural boundaries are evolved during topology optimization. Since 1988, when the concept of topology optimization was first proposed by Bendsøe and Kikuchi [4], a broad spectrum of topology optimization studies have been carried out, mainly for structural design problems such as maximum stiffness problems and compliant mechanism design problems. More recently, topology optimization techniques have been extended to electromagnetic wave propagation problems. Chung et al. [5] carried out studies on the design of microlenses, using topology optimization based on a density method, in which lenses were optimized for relatively near focal points lying in the fixed design domain. However, their method can only be applied to problems with focal points in the analysis region, and does not take viewing angles or resolutions into account.

In this study, we propose a new far-infrared lens design method using topology optimization in which the directivity in the far-field is optimized by using the electric field distribution in the near-field, which

enables the optimal design of lenses given only a desired directivity pattern. To verify the effectiveness of the proposed method, we optimize a light collimator design. Furthermore, although silicon absorbs far-infrared electromagnetic radiation emitted from live sources such as the human body to a small degree, we employ silicon as the far-infrared lens material because it is more economical than the germanium that is most often used in such applications. The optimization algorithm uses the finite element method (FEM) for solving the equilibrium and adjoint equations, and the design problem is formulated as a two-dimensional case. The outline of this paper is as follows. The concept of the topology optimization method is explained in Section 4. In Section 5 and 6, the optimization problem for the design of the far-infrared lens is formulated using the density method. Next, sensitivity analysis using the adjoint variables method is explained in Section 7, and numerical implementations are explained in Section 8. Finally, in Section 9. numerical examples of optimally designed far-infrared lens structures are presented.

4. Concept of topology optimization method and application to electromagnetic problems

Here, we briefly discuss the concept of the proposed topology optimization method and how to address the electromagnetic problem. In this research, we apply topology optimization to the design of a dielectric substance to create a far-infrared lens capable of collimating electromagnetic waves that are propagated from a point source. The key idea of topology optimization methods is the introduction of a fixed, extended design domain D that includes the original design domain Ω_d, and the use of the following characteristic function, as follows:

$$\begin{cases} \chi_\Omega(\boldsymbol{x}) = 1 \quad \text{if} \quad \boldsymbol{x} \in \ \Omega_d \\ \\ \chi_\Omega(\boldsymbol{x}) = 0 \quad \text{if} \quad \boldsymbol{x} \in \ D \backslash \Omega_d, \end{cases} \tag{1}$$

where $\boldsymbol{x}$ denotes a position in the extended design domain D. Figure 1 shows the relation between the extended design domain D and the original design domain Ω_d. Using this characteristic function, the original structural design problem is replaced by a material distribution problem. Since this characteristic function can be very discontinuous, i.e., resides in $L^\infty(D)$, some regularization or smoothing technique must be introduced for the numerical treatment. Several methods such as the homogenization method [6] and the density method [7] have been utilized for the relaxation of the domain. In this research, the density method is employed, due to its simple formulation for cases where the material property has an isotropic response.

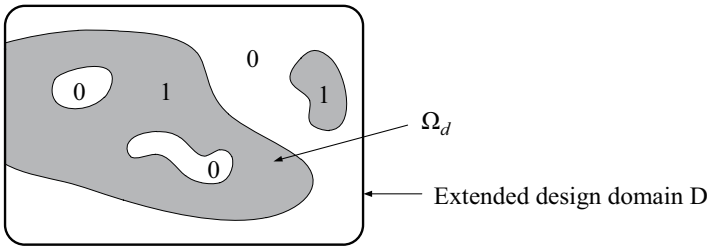

Fig. 1: Concept of topology optimization

In electromagnetic wave propagation problems, the electric permittivity and the magnetic permeability are the physical properties that determine wave propagation phenomena. Here, however, the magnetic permeability can be regarded as a constant during the optimization, since its value for dielectric materials such as the silicon used in this application is almost the same as that of voids filled with air. Furthermore, these dielectric materials typically show isotropic responses, and their relative permittivity can be expressed as a real scalar value. Therefore, based on the density method, the relative permittivity ϵ_r is described as

$$\epsilon_r(\rho(\boldsymbol{x})) = \epsilon_r^{\text{air}} + (\epsilon_r^{\text{dielectric}} - \epsilon_r^{\text{air}})\rho(\boldsymbol{x}), \tag{2}$$

where $\rho(\boldsymbol{x})$ is the normalized density such that

$$0 \leq \rho(\boldsymbol{x}) \leq 1, \tag{3}$$

and ϵ_r^{air} and $\epsilon_r^{\text{dielectric}}$ are the relative permittivity in air and the dielectric material, respectively. Equation (2) is a successive approximation equation that can be used to represent physical phenomena. Here, the

density ρ is used for the design variables in the optimal design problem.

5. Formulation of electromagnetic wave propagation problem

The wave propagation equations for electromagnetic fields are derived from Maxwell's equation by transforming it to the frequency domain. That is, by assuming a periodic response of the electric and magnetic fields, respectively $\boldsymbol{E}$ and $\boldsymbol{H}$, with a radian frequency ω, we obtain

$$\nabla\times\boldsymbol{E} = -j\omega\mu\boldsymbol{H}, \quad \text{and} \tag{4}$$

$$\nabla\times\boldsymbol{H} = j\omega\epsilon\boldsymbol{E}, \tag{5}$$

where j is an imaginary number, and ϵ and μ are the electric permittivity and magnetic permeability, respectively. Here, we assume that the dielectric substrate has an isotropic response. By eliminating the magnetic field $\boldsymbol{H}$ in Eq.(4), the following Helmholtz equation is obtained:

$$\nabla\times\frac{1}{\mu_r}(\nabla\times\boldsymbol{E}) - k_0^2\epsilon_r\boldsymbol{E} = 0, \tag{6}$$

where k_0 is the wave number such that $k_0 = \omega\sqrt{\epsilon_0\mu_0}$, ϵ_0 and μ_0 are the electric permittivity and magnetic permeability of air, respectively, and ϵ_r and μ_r are the relative permittivity and relative permeability of the dielectric material, respectively. Since the magnetic permeability values for the dielectric material and the voids filled with air are practically the same, the relative permeability μ_r is set to 1 in the above equation and the following equation is obtained:

$$\nabla\times(\nabla\times\boldsymbol{E}) - k_0^2\epsilon_r\boldsymbol{E} = 0. \tag{7}$$

Eq.(7) is the governing equation of electromagnetic wave propagation problems. In this paper, the design problem is formulated for a two-dimensional case, and we confine our analysis to transverse electric (TE) waves (Fig. 2).

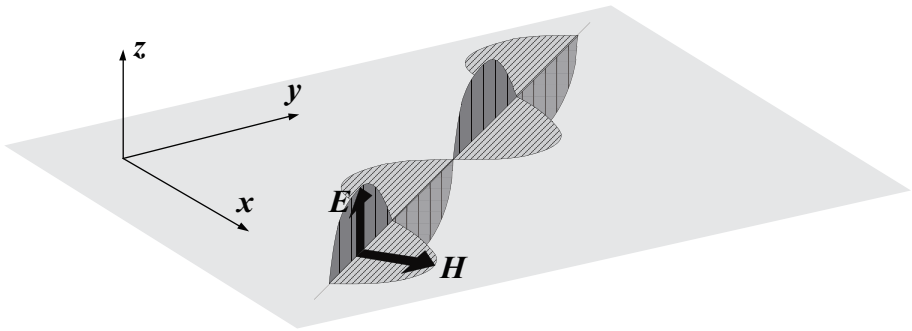

Fig. 2: TE wave

TE waves propagate in the x-y direction where the electric field vector is polarized orthogonal to the direction of wave propagation, and the direction of the wave amplitude is in the z-direction. Thus, Eq.(8) is rewritten as follows:

$$\nabla^2 E_z + k_0^2\epsilon_r E_z = 0. \tag{8}$$

6. Formulation of optimization problem

Next, we describe the formulation of the objective function. In this study, using the electric field distribution in the near-field, we aim to obtain a far-infrared lens design that collimates electromagnetic waves propagated from a point source, as shown in Fig. 3.

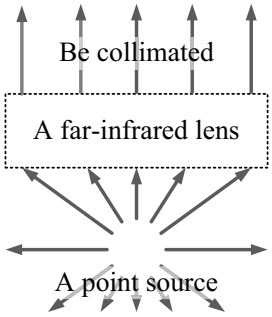

Fig. 3: Collimated electromagnetic waves

To model the electromagnetic wave collimation, we prepare two analysis modes. In the first mode, termed the "optimization mode," electromagnetic waves radiated from a point source are collimated. In the second mode, termed the "reference mode," the electric field distribution of incident plane waves propagating from the lower boundary of the analysis region are analyzed, as shown in Fig. 4.

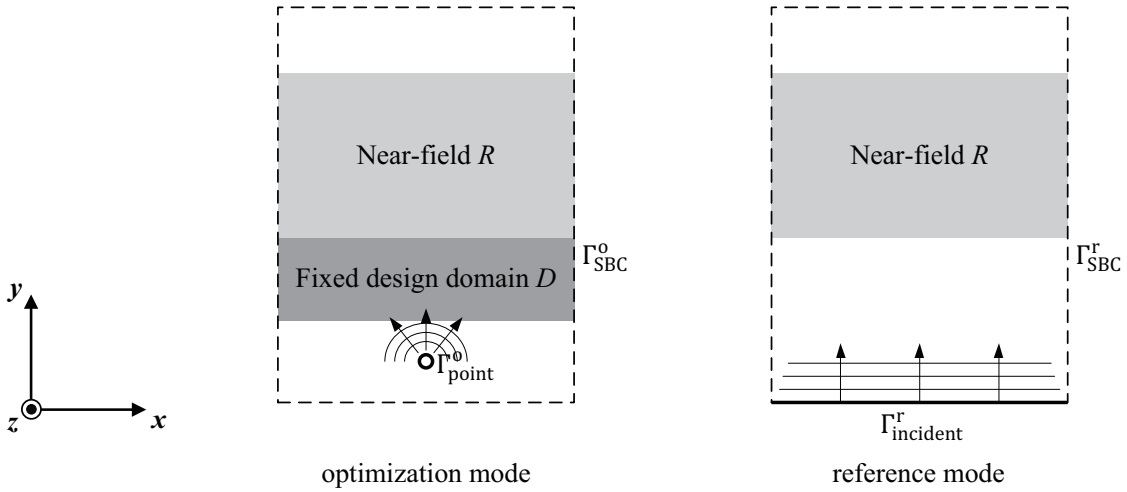

Fig. 4: Two modes and boundary condition

By adjusting the electric field distribution of the optimization mode so that it approaches that of the reference mode in the near-field, the directivities of the two modes in the far-field are made to approach congruence. Therefore, we set the objective function to minimize the integral of the absolute value of the difference between the z-components of the electric field in the two modes over the region that is defined as the near-field. The objective function is defined as follows:

$$\inf_{\rho} \quad \int_R (E_z^{\mathrm{o}} - E_z^{\mathrm{r}})(E_z^{\mathrm{o}*} - E_z^{\mathrm{r}*}) dR, \tag{9}$$

where R is the region that is defined as the near-field, and E_z^o and E_z^r are the z-components of the electric field in the optimization mode and reference mode, respectively. Although a single reference mode is used in this study, multiple reference modes can be easily implemented and adapted to particular design problems in order to optimize lens designs for a variety of devices.

Boundary conditions are given as follows:

$$\boldsymbol{n} \cdot (\nabla E_z^{\mathrm{o}}) + jk_0 E_z^{\mathrm{o}} = 0 \qquad \text{on} \quad \Gamma^{\mathrm{o}}_{\mathrm{SBC}}, \tag{10}$$

$$E_z^{\mathrm{o}} = E_{z0}^{\mathrm{o}} \qquad \text{on} \quad \Gamma^{\mathrm{o}}_{\mathrm{point}}, \tag{11}$$

$$\boldsymbol{n} \cdot (\nabla E_z^{\mathrm{r}}) + jk_0 E_z^{\mathrm{r}} = 0 \qquad \text{on} \quad \Gamma^{\mathrm{r}}_{\mathrm{SBC}}, \tag{12}$$

$$\boldsymbol{n} \cdot (\nabla E_z^{\mathrm{r}}) + jk_0 E_z^{\mathrm{r}} = 2jk_0 E_{z0}^{\mathrm{r}} \qquad \text{on} \quad \Gamma^{\mathrm{r}}_{\mathrm{incident}}. \tag{13}$$

where $\boldsymbol{n}$ is the normal direction vector of a boundary, and E^{o}_{z0} and E^{r}_{z0} are given as the z-components of the electric field on $\Gamma^{\mathrm{o}}_{\mathrm{point}}$ in the optimization mode and on $\Gamma^{\mathrm{r}}_{\mathrm{incident}}$ in the reference mode, respectively, and $\Gamma^{\mathrm{o}}_{\mathrm{point}}$ and $\Gamma^{\mathrm{r}}_{\mathrm{incident}}$ are boundaries for radiating electromagnetic waves as a point source and making a incident plane wave, respectively, $\Gamma^{\mathrm{o}}_{\mathrm{SBC}}$ and $\Gamma^{\mathrm{r}}_{\mathrm{SBC}}$ are boundaries for absorbing electromagnetic waves, scattering boundary conditions (SBC). Scattering boundary conditions imposed in order to avoid the effects of unrelated electromagnetic waves and ensure that absorption is established outside the analysis region.

In this study, we use a penalty function to avoid the presence of grayscale areas in the optimized configurations. Grayscales are areas where the design variables ρ have an intermediate value between 0 and 1. The inclusion of such areas if the optimized configurations is undesirable from an engineering point of view, due to the impossibility of manufacturing such configurations. The penalty function is applied to the design variables ρ and is described as:

$$P(\rho) = \int_D \frac{1}{2}\big\{1 - \cos(2\pi\rho)\big\} d\Omega. \tag{14}$$

By minimizing $P(\rho)$, the integral over the fixed design domain D, the design variables ρ are made to approach values of 0 or 1. The penalty function added to the objective function is multiplied by a parameter, τ, which represents the strength of the penalty, and both functions are simultaneously minimized by adjusting the value of τ. Thus, the optimization problem for the minimization of the resolution is formulated as follows:

$$\inf_{\rho} \quad F(E^{\mathrm{o}}_z, E^{\mathrm{r}}_z, \rho) = \int_R (E^{\mathrm{o}}_z - E^{\mathrm{r}}_z)(E^{\mathrm{o}*}_z - E^{\mathrm{r}*}_z) dR + \tau P(\rho), \tag{15}$$

$$\text{subject to} \quad a_1(E^{\mathrm{o}}_z, E^{\mathrm{r}}_z, \tilde{E}_z, \rho) + a_2(E^{\mathrm{o}}_z, E^{\mathrm{r}}_z, \tilde{E}_z) = l(\tilde{E}_z), \tag{16}$$

$$\epsilon_r(\rho(\boldsymbol{x})) = \epsilon^{\mathrm{air}}_r + (\epsilon^{\mathrm{silicon}}_r - \epsilon^{\mathrm{air}}_r)\rho(\boldsymbol{x}), \tag{17}$$

$$0 \le \rho(\boldsymbol{x}) \le 1, \tag{18}$$

where, $\tilde{E}_z$ are a test function, and

$$\begin{aligned} a_1(E^{\mathrm{o}}_z, E^{\mathrm{r}}_z, \tilde{E}_z, \rho) = &\int_{\Omega_o} \nabla E^{\mathrm{o}}_z \cdot \nabla \tilde{E}_z d\Omega - k_0^2 \int_{\Omega_o} \epsilon_r(\rho) E^{\mathrm{o}}_z \tilde{E}_z \, d\Omega \\ &+ \int_{\Omega_r} \nabla E^{\mathrm{r}}_z \cdot \nabla \tilde{E}_z d\Omega - k_0^2 \epsilon^{air}_r \int_{\Omega_r} E^{\mathrm{r}}_z \tilde{E}_z d\Omega, \end{aligned} \tag{19}$$

$$\begin{aligned} a_2(E^{\mathrm{o}}_z, E^{\mathrm{r}}_z, \tilde{E}_z) = &jk_0 \int_{\Gamma^{\mathrm{o}}_{\mathrm{SBC}}} E^{\mathrm{o}}_z \tilde{E}_z \, d\Gamma \\ &+ jk_0 \int_{\Gamma^{\mathrm{r}}_{\mathrm{SBC}} \cup \Gamma^{\mathrm{r}}_{\mathrm{incident}}} E^{\mathrm{r}}_z \tilde{E}_z d\Gamma, \end{aligned} \tag{20}$$

$$l(\tilde{E}_z) = 2jk_0 E^{\mathrm{r}}_{z0} \int_{\Gamma^{\mathrm{r}}_{\mathrm{incident}}} \tilde{E}_z d\Gamma, \tag{21}$$

where, Ω_o and Ω_r are the entire area analyzed of optimization mode and reference mode, respectively.

7. sensitivity analysis

In this study, we analyze sensitivity using the adjoint variable method. First, we formulate the lagrangian of the optimization problem as follows:

$$\bar{F} = F(E^{\mathrm{o}}_z, E^{\mathrm{r}}_z, \rho) - \big\{a_1(E^{\mathrm{o}}_z, E^{\mathrm{r}}_z, \tilde{E}_z, \rho) + a_2(E^{\mathrm{o}}_z, E^{\mathrm{r}}_z, \tilde{E}_z) - l(\tilde{E}_z)\big\}, \tag{22}$$

where $\tilde{E}_z$ represent an adjoint variable. The gradient of the lagrangian is given as follows:

$$\begin{aligned} \bar{F}' = &F(E^{\mathrm{o}\prime}_z, E^{\mathrm{r}}_z, \rho) + F(E^{\mathrm{o}}_z, E^{\mathrm{r}\prime}_z, \rho) + F(E^{\mathrm{o}}_z, E^{\mathrm{r}}_z, \rho') \\ &-\{a_1(E^{\mathrm{o}\prime}_z, E^{\mathrm{r}}_z, \tilde{E}_z, \rho) + a_1(E^{\mathrm{o}}_z, E^{\mathrm{r}\prime}_z, \tilde{E}_z, \rho) + a_1(E^{\mathrm{o}}_z, E^{\mathrm{r}}_z, \tilde{E}_z{}', \rho) + a_1(E^{\mathrm{o}}_z, E^{\mathrm{r}}_z, \tilde{E}_z, \rho') \\ &+a_2(E^{\mathrm{o}\prime}_z, E^{\mathrm{r}}_z, \tilde{E}_z) + a_2(E^{\mathrm{o}}_z, E^{\mathrm{r}\prime}_z, \tilde{E}_z) + a_2(E^{\mathrm{o}}_z, E^{\mathrm{r}}_z, \tilde{E}_z{}') - l(\tilde{E}_z{}')\}. \end{aligned} \tag{23}$$

In the above equation adjoint variables have the following relation:

$$a_1(E_z^{\mathrm{o}}, E_z^{\mathrm{r}}, \tilde{E}_z{}', \rho) + a_2(E_z^{\mathrm{o}}, E_z^{\mathrm{r}}, \tilde{E}_z{}') - l(\tilde{E}_z{}') = 0. \tag{24}$$

The electric field of the reference mode, E_z^{r}, is not a function of the density ρ, and the following equation obtained:

$$F(E_z^{\mathrm{o}}, E_z^{\mathrm{r}\prime}, \rho) = a_1(E_z^{\mathrm{o}}, E_z^{\mathrm{r}\prime}, \tilde{E}_z, \rho) = a_2(E_z^{\mathrm{o}}, E_z^{\mathrm{r}\prime}, \tilde{E}_z) = 0. \tag{25}$$

Next, we cancel out the differential for the state variable, to set the adjoint field as follows:

$$F(E_z^{\mathrm{o}\prime}, E_z^{\mathrm{r}}, \rho) + a_1(E_z^{\mathrm{o}\prime}, E_z^{\mathrm{r}}, \tilde{E}_z, \rho) + a_2(E_z^{\mathrm{o}\prime}, E_z^{\mathrm{r}}, \tilde{E}_z) = 0. \tag{26}$$

By using the adjoint variables obtained by solving the above formula, the adjoint equation, the sensitivity is obtained as follows:

$$\bar{F}' = F(E_z^{\mathrm{o}}, E_z^{\mathrm{r}}, \rho') - a_1(E_z^{\mathrm{o}}, E_z^{\mathrm{r}}, \tilde{E}_z, \rho'). \tag{27}$$

8. Numerical implementations

In this section, we first explain the optimization algorithm based on the formulations shown in Section 6. Fig. (5) shows a flowchart of the optimization, which has five steps in the per-iteration loop. As shown in this figure, model data is first input via the COMSOL Multiphysics GUI (COMSOL), since it facilitates constructing and analyzing models that have complicated shapes and physical constraints. The optimization algorithm is implemented using the MATLAB scripting language. Next, the electric field is analyzed for the model using the FEM and the objective function. The optimization process terminates if the objective function is converged, otherwise the sensitivities of the objective function are calculated based on the adjoint variable method. The design variables are then updated using the calculated sensitivities and Sequential Linear Programming (SLP). After updating the densities of the dielectric material using the updated design variables, the procedure returns to the first step of the iteration loop.

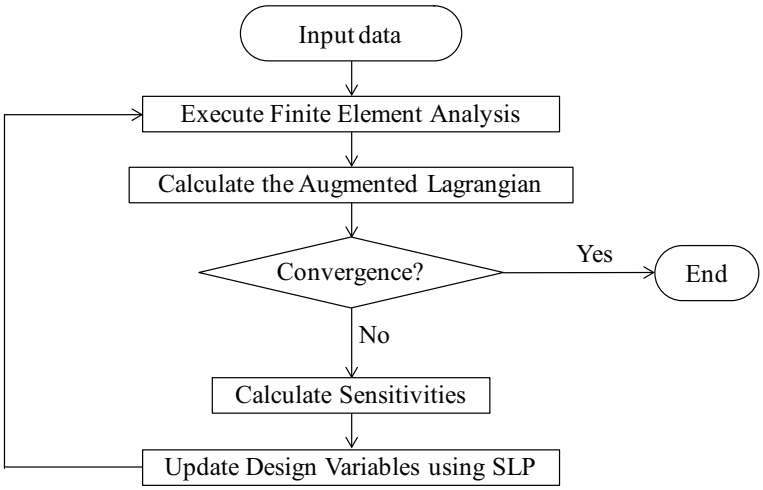

Fig. 5: Flowchart of the optimization algorithm

9. Numerical example

Here, we present a numerical example to confirm the usefulness of the proposed method. We consider the design of the far-infrared lens structure shown in Fig. 3 and set the geometrical parameters as shown in Fig. 6.

The relative permittivity in air and in silicon, $\epsilon_r^{\mathrm{air}}$ and $\epsilon_r^{\mathrm{silicon}}$, are respectively set to 1.0 and $11.7 + i \times 5.79 \times 10^{-4}$. The relative permittivity of materials such as silicon is called a complex permittivity, with the imaginary term related to the absorption of electromagnetic waves. The frequency of electromagnetic waves radiating from a point source and propagating as a plane wave is set to 10 µm, roughly the same wavelength as the electromagnetic waves radiated from the human body. The z-components of the electric field on $\Gamma_{\mathrm{point}}^{\mathrm{o}}$ in the optimization mode and on $\Gamma_{\mathrm{incident}}^{\mathrm{r}}$ in the reference mode, E_{z0}^{o} and E_{z0}^{r}, are 250 V/m and 100 V/m, respectively. The fixed design domain is divided into 1,200 (20×60) design elements for the topology optimization.

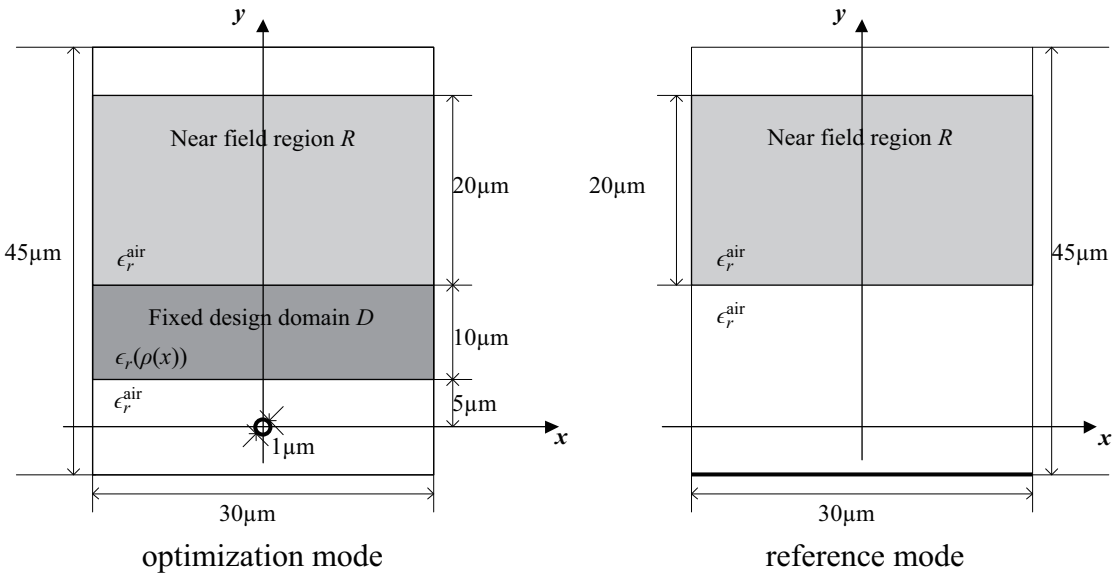

Fig. 6: Geometrical parameters

The parameter τ is to adjust the weight of the penalty function P for the objective function F. Therefore, it can not be determined uniquely without parametric study. We obtain several structures of a far-infrared lens by preparing several parameters τ, which are considered adjustment of a ratio of a value of the objective function with respect to the initial value of the density ρ for that of the penalty function. We perform parametric study sufficiently to obtain a optimal configuration. Figure 7 shows the density distribution of the silicon of the optimal configuration and three other configurations which is not optimal For some reason.

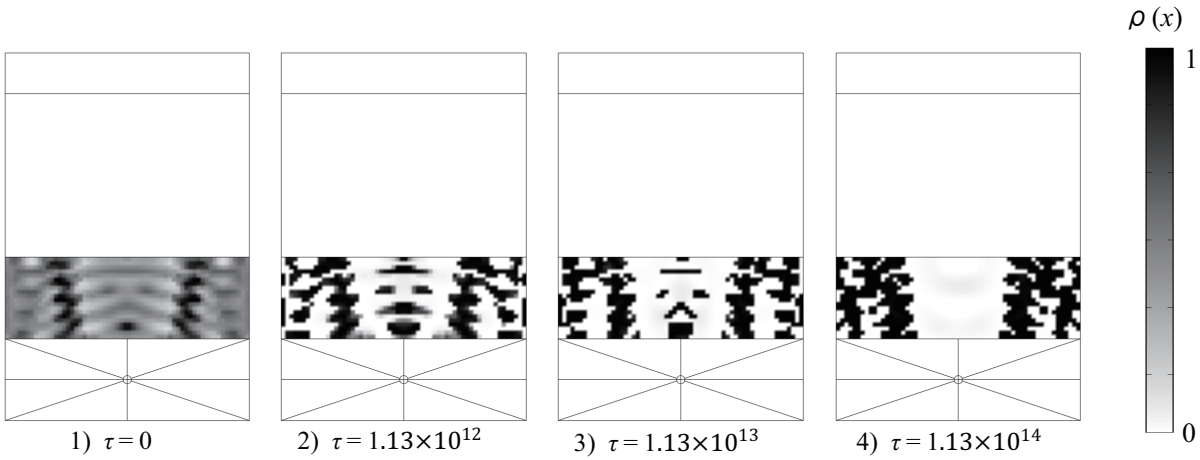

Fig. 7: Optimal density distribution

The white areas indicate air and the black areas indicate locations where the silicon is fully present. On the other hand, the gray area, grayscale, don't indicate air or the silicon and is a feasible area from an engineering perspective. In Fig. 7, the configurations when τ are 0 and 1.13×10^{12} contain grayscale, thus they are not optimal. On the other hand, the configurations when τ are 1.13×10^{13} and 1.13×10^{14}, grayscale are not contained, and have clear optimal configurations. On the other hand, we explain the far-field of the two clear optimal configurations, in addition to plane wave and wave radiated from a point source, shown in Fig. 8.

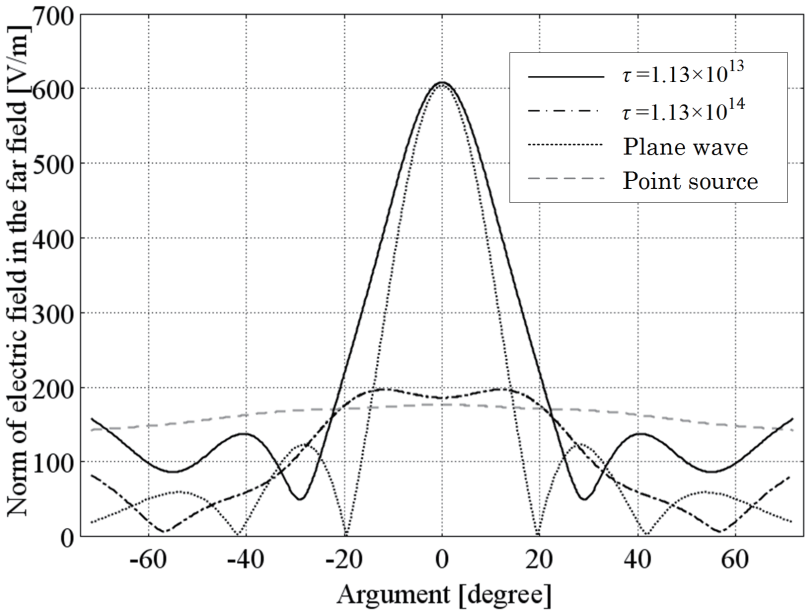

Fig. 8: Graph of far-field comparison

The horizontal and vertical axis in Fig. 8 are the argument and the norm of the electric field in the far field. The range of argument of the horizontal axis is where to receive not a little influence of the lens. In Fig. 8, when τ is 1.13 $\times 10^{13}$ the norm of the electric field in the far field of optimization mode is similar to reference mode, but when τ is 1.13 $\times 10^{14}$ it is not similar. Therefore, the configuration when τ is 1.13 $\times 10^{14}$ is not satisfied desired properties. Finally, fig. 9 represent the distribution of z-component of the electric field for both modes.

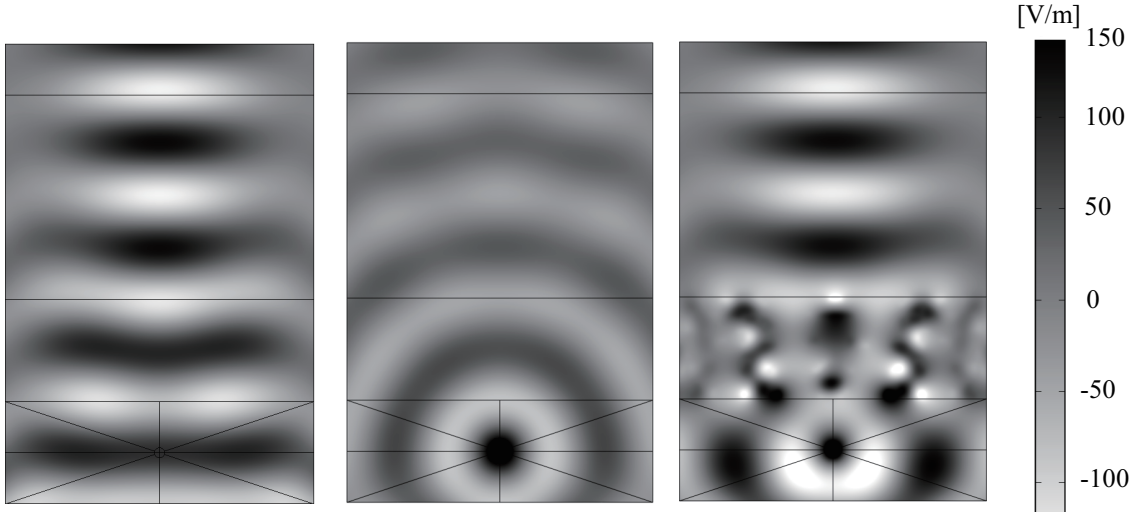

Fig. 9: Distribution of electric field z-component for both modes

The above figure shows that the distribution on the near-field of the optimization mode is almost the same as that of the reference mode. In other words, electromagnetic waves radiated from a point source, is collimated and is acting like a plane wave. Therefore, the solution indicates that the proposed method has generated a clear optimal configuration.

10. Conclusion

We developed a topology optimization method for the design of a far-infrared lens structure composed of silicon. The optimization problem was formulated to obtain an effective optimal solution by specifying a new objective function so that the desired performance characteristics could be achieved. The density method was used to avoided grayscales in the optimal configurations. The optimization algorithm was constructed based based on the developed formulations using COMSOL and MATLAB software. Finally, a numerical example of an optimally designed far-infrared lens structure was provided to confirm the usefulness of proposed method.

11. References

[**1**] H. Saito, T. Hagihara, K. Hatanaka and T. Sawai, Development of pedestrian detection system using far-infrared ray camera, *SEI Technical Review*, No. 66, pp. 112-117, 2008.

[**2**] M. Aoki and N. Yasuda, Pedestrian detection using on-board far-infrared cameras, *Transactions of Information Processing Society of Japan*, Vol. 47, No. 5, pp. 1-9, 2006.

[**3**] O. Tsimhoni, J. Bargman, T. Minoda, and M. J. Flannagan, Pedestrian detection with near and far infrared night vision enhancement, *University of Michigan Transportation Research Institute Technical Report*, Vol. 38, pp. 1-25, 2004.

[**4**] K. Kidono, A. Takahashi, Y. Ninomiya, Reliable pedestrian detection using a laser scanner, *Institute of Electronics, Information, and Communication Engineers*, pp. 300, 2006.

[**5**] Y. S. Chung, B. Lee and S. Kim, Optimal shape design of dielectric micro lens using FDTD and topology optimization, *Journal of the Optical Society of Korea*, Vol.13, No.2, pp. 286-293, 2009.

[**6**] K. Suzuki and N. Kikuchi, RA homogenization method for shape and topology optimization, *Computer Methods in Applied Mechanics and Engineering*, Vol. 93, No. 3, pp. 291-318, 1991.

[**7**] R. J. Yang and C. H. Chuang, Optimal topology design using linear-programming, *Computers and Structures*, Vol. 52, No. 2, pp. 265-275, 1994.

[**8**] M. Otomori, T. Yamada, K. Izui, S. Nishiwaki and N. Kogiso, Level Set-Based Topology Optimization for the Design of a Ferromagnetic Waveguide, *IEEE Transactions On Magnetics*, Vol. 48, No. 11, pp. 3072-3075, 2012.